

Real–World Considerations for Deep Learning in Wireless Signal Identification Based on Spectral Correlation Function

Kürşat Tekbıyık, *Student Member, IEEE*, Özkan Akbunar, *Student Member, IEEE*,
Ali Rıza Ekti, *Member, IEEE*, Ali Görçin, *Senior Member, IEEE*, Güneş Karabulut Kurt, *Senior Member, IEEE*

Abstract—This paper proposes a convolutional neural network (CNN) model which utilizes the spectral correlation function (SCF) for wireless radio access technology identification without any prior information about bandwidth and/or the center frequency. The sensing and classification methods are applied on the baseband equivalent signals. Two different approaches are elaborated. The proposed method is implemented in two different settings; in the first setting signals are jointly sensed and classified. Sensing and classification are conducted in a sequential manner in the second setting. The performance of both approaches are discussed in detail. The proposed method eliminates threshold estimation processes of classical estimators. It also eliminates the need to know distinct features of signals beforehand. Over-the-air real-world measurements are used to show the robustness and the validity of the proposed method and various wireless signals are successfully distinguished from each other without any a priori knowledge. The over-the-air real-world measurements are also shared in the format of SCF. The performance of SCF-based identification is compared with the cases when fast Fourier transform and amplitude–phase representation are used as the training inputs for CNN. The comparative performance of the proposed method is quantified by precision, recall, and F1-score metrics. Moreover, a setup to compare the performance of the proposed approach with classical cyclostationary features detection (CFD) is prepared. Measurement results indicate the superiority of the proposed method against CFD, especially at the low signal-to-noise ratio regime.

I. INTRODUCTION

In addition to being an established method for spectrum sensing in cognitive radio domain, cyclostationary feature detection (CFD) is also utilized to distinguish generic modulation techniques such as M–PSK, M–FSK, and M–QAM [1]. When the radio access technology (RAT) identification is considered [2], second order cyclostationarity is employed

This manuscript has been submitted for the possible publication in the IEEE Transactions on Cognitive Communications and Networking (TCCN). It is currently under review.

K. Tekbıyık, Ö. Akbunar, A. Görçin and A.R. Ekti are with Informatics and Information Security Research Center (BİLGEM), TÜBİTAK, Kocaeli, Turkey. e-mail: {kursat.tekbıyık, ali.gorcin, ozkan.akbunar, aliriza.ekti}@tubitak.gov.tr

A.R. Ekti is with the Department of Electrical–Electronics Engineering, Balıkesir University, Balıkesir, Turkey. e-mail: arekti@balikesir.edu.tr

A. Görçin is with the Department of Electronics and Communications Engineering, Yıldız Technical University, İstanbul, Turkey. e-mail: agorcin@yildiz.edu.tr

K. Tekbıyık and G.K. Kurt are with the Department of Electronics and Communications Engineering, İstanbul Technical University, İstanbul, Turkey. e-mail: {tekbıyık, gkurt}@itu.edu.tr

for classification of Long–Term Evolution (LTE) and Global System for Mobile communications (GSM) signals [3]. Later, a tree-based classification approach is proposed to identify GSM, cdma2000, universal mobile telecommunications system (UMTS), and LTE signals [4]. These classical identification techniques depend on extracting the underlying features using likelihood–based techniques and statistical decision mechanisms. Therefore, their decision parameters such as thresholds and the number of required samples need to be adjusted in an adaptive manner under dynamically changing real-life conditions [5].

Recently, deep learning (DL) has been proposed as a solution to the parameter adaptation issues of classical techniques. This stems from the known ability of DL techniques in extracting the intrinsic features of given inputs through a convolutional process. The use of DL based approaches eliminates the need for a statistical decision mechanism at the end of the identification process. Along this line, the recent study shows that DL methods outperform classical approaches in signal detection in the spectrum [6]. Furthermore, convolutional neural networks (CNNs) are trained with high–order statistics of single carrier signals for modulation classification [7].

A CNN classifier is used for modulation and interference identification for industrial scientific medical (ISM) bands by utilizing fast Fourier transform (FFT), amplitude–phase representation (AP) and in–phase/quadrature (I/Q) features for training [8]. Another study [9] focuses on the protocol classification in ISM band by utilizing fully connected neural networks. As another example of the application of DL to signal classification, long short term memory (LSTM) is deployed for modulation classification and identification of digital video broadcast (DVB), Tetra, LTE, GSM, wide–band FM (WFM) signals by using AP and FFT magnitude for training [10]. Recently, DL networks are used to identify the cellular communication signals in Rayleigh fading channels [11]. The classification performance of the proposed model is high, however, it employs synthetic data generated by using Matlab. In the real channels, there are numerous phenomenons, which further complicate the signal characteristics. It is also worth mentioning that research is now available in the literature on how signal classifiers perform when exposed to possible adversarial attacks. For example, in [12], it is shown using different databases that adversarial attacks reduce the performance of the signal classifier.

In our previous study [13], we employed real–life signals

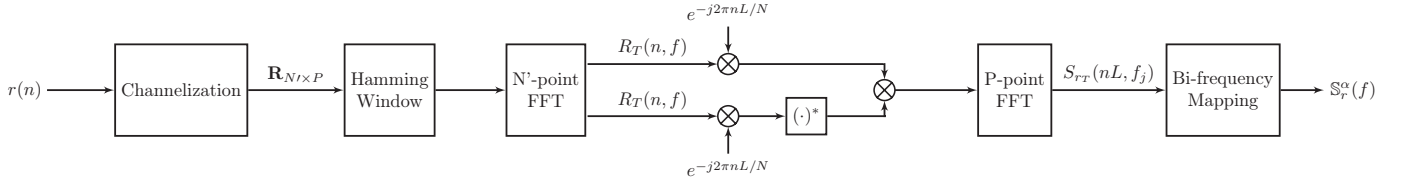


Fig. 1. Six steps of the FAM algorithm: Channelization, windowing, first FFT, complex multiplication, second FFT, and mapping.

to train and test the support vector machine (SVM). In the study, spectral correlation function (SCF) is utilized as feature vector. Even though SVM gives high performance by using SCF of signals, the computation of SCF is complex owing to the bi-frequency mapping in FFT accumulation method (FAM). Therefore, the hardware cost and consumption of time is considerable.

In this study, a new CNN method, which is trained utilizing the SCFs of wireless without bi-frequency mapping, is proposed for spectrum sensing and signal identification. Thus, such an approach leads to reduction in terms of complexity when compared to the previous works and can be utilized either to decide whether the signal is present or not or to distinguish GSM, UMTS, and LTE signals from each other. The superiority of SCF as a training feature is shown by comparing its performance against AP and FFT. The performance of the proposed method is also compared with cyclostationary features detection (CFD), which requires the cyclic frequencies as a priori information. The comparison is done based on real-world measurements taken during an extensive measurement campaign conducted at different locations with varying environmental conditions in terms of the channel fading statistics and signal-to-noise ratio (SNR) levels. The dataset composed real-world measurements is also shared in [14] in the format of SCF, which is the main method used in this study. The identification results indicate the superiority of the proposed method over the aforementioned ones. Although the utilization of SCF based CNNs to identify wireless RATs without any a priori information is the main contribution of this paper, the scope of this work can be extended to the identification of any signal, which exhibits cyclostationary features.

The remainder of this paper is structured as follows. Background information on the system model, cyclostationary analysis and CNNs is presented in Section II. The proposed CNN model is given in Section III. The problem statement is discussed in Section IV. The details of the dataset used in this study are drawn in Section V. Section VI presents the classification performance of the proposed method. The concluding remarks are provided in Section VII.

II. BACKGROUND

As all process is carried out in the baseband, firstly we need to define the complex baseband equivalent of the received signal, $r(t)$. When the presence of fading environment with thermal noise, it can be given as

$$r(t) = \rho(t) * x(t) + \omega(t), \quad (1)$$

where $\omega(t)$ denotes the complex additive white Gaussian noise (AWGN) with $\mathcal{C} \sim N(0, \sigma_N^2)$ in the form of $\omega(t) = \omega_I(t) +$

$j\omega_Q(t)$ as both $\omega_I(t)$ and $j\omega_Q(t)$ being $\mathcal{C} \sim N(0, \sigma_N^2/2)$ and $j = \sqrt{-1}$; the complex baseband equivalent of the transmitted signals is denoted as $x(t)$; and $\rho(t)$ stands for the impulse response for the time-invariant wireless channel because of extremely short observation time for a signal.

Depending on the idle or busy state of the mobile propagation channel of radio frequency (RF) spectrum with the presence of the transmitted signal, the signal detection by utilizing deep learning methods can be shown as a binary hypothesis test

$$r(t) = \begin{cases} \rho(t)x(t) + \omega(t), & H_1 \\ \omega(t), & H_0. \end{cases} \quad (2)$$

H_0 and H_1 are the hypotheses respect to presence of noise only and the unknown signal, respectively. Therefore, the problem statement can be stated as identification of the presence of the unknown signal $x(t)$ and $\omega(t)$ and classify the unknown transmitted signal.

A. Cyclostationarity

Cyclostationary signal processing leads to extracting hidden periodicities in a received signal, $r(t)$. Since these periodicities (e.g., symbol periods, spreading codes, and guard intervals) exhibit unique characteristics for different signals, they provide the necessary information for identification. Thus, the unknown signals $x(t)$ can be identified by using cyclostationary features to obtain the statistical characteristics of $r(t)$ in the presence of $\omega(t)$ and multipath fading without a priori information. A nonlinear transformation, second-order cyclostationarity of a signal can be expressed as

$$s_\tau(t) = \mathbb{E} \{ r(t + \tau/2)r^*(t - \tau/2) \}, \quad (3)$$

where $s_\tau(t)$ is the autocorrelation of $r(t)$. Assuming that the autocorrelation function is periodic with T_0 for second-order cyclostationary signals, a Fourier series expansion of $s_\tau(t)$ is

$$\mathbb{R}_r^\alpha(\tau) = \frac{1}{T_0} \int_{-T_0/2}^{T_0/2} s_\tau(t) e^{-j2\pi\alpha t} dt, \quad (4)$$

where $\mathbb{R}_r^\alpha(\tau)$ is the cyclic autocorrelation function (CAF) and α values are the cyclic frequencies.

The Fourier transform of the CAF for a fixed α is given with the cyclic Wiener relation [1]

$$\mathbb{S}_r(f) = \int_{-T/2}^{T/2} \mathbb{R}_r^\alpha(\tau) e^{-j2\pi f\tau} d\tau, \quad (5)$$

where $\mathbb{S}_r(f)$ is called as SCF which is equal to the power spectral density (PSD) when α is zero.

The computational complexity of calculating SCF is relatively high. However, this complexity can be decreased by using the FAM based on time smoothing via FFT [15]. FAM estimates the SCF as

$$\mathbb{S}_{r_T}^{\alpha_i+q\Delta\alpha}(nL, f) = \sum_k R_T(kL, f)R_T^*(kL, f) \cdot g_c(n-k)e^{-i2\pi kq/P}, \quad (6)$$

where $R_T(n, f)$ denotes the complex demodulates which is the N' -point FFT of $r(n)$ passed through a Hamming window and can be computed by

$$R_T(n, f) = \sum_{k=-N'/2}^{N'/2} a(k)r(n-k)e^{-i2\pi f(n-k)T_s}, \quad (7)$$

where $a(n)$ and $g_c(n)$ are both data tapering windows. The block diagram of FAM is depicted in Fig. 1. The symbols N' , T_s , and L denotes the channelization length, sampling period, and sample size of hopping blocks, respectively. The ratio between the number of total samples and L is employed as the length of second FFT, whose length is denoted as P . The FAM has six implementation steps. These steps are respectively channelization, windowing, N' -point FFT, complex multiplication, P -point FFT and bi-frequency mapping. The most computationally complex step among them is bi-frequency mapping. Therefore, as will be detailed in the later, the bi-frequency mapping is omitted and the matrix before this step is used as a feature. In the study, the unit rectangle and Hamming windows are employed as $g_c(n)$ and $a(n)$, respectively. Fig. 2 illustrates SCFs results in bi-frequency plane, which are estimated by FAM algorithm for GSM, UMTS, and LTE.

Please note that the bi-frequency mapping step is bypassed to reduce the complexity and time consumption in the FAM algorithm. As a result, the input matrix, \mathbf{X}_k^{SCF} , to be fed into classifier model is given as

$$\mathbf{X}_k^{SCF} = |\mathbb{S}_{r_T}(nL, f)|, \quad (8)$$

In this paper, we use the Keras library in Python for training and running the CNNs. Similar to the other existing machine learning classifiers, this library does not support complex-valued classification. Therefore, the use of the SCF is restricted to its magnitude, as shown in (8).

B. Amplitude-Phase

The amplitude and phase values of time-domain I/Q data can be used to establish a real-valued classification feature matrix, \mathbf{X}_k^{AP} . This feature matrix is composed of the amplitude and phase vectors of the received signal samples. So, \mathbf{X}_k^{AP} is defined as

$$\mathbf{X}_k^{AP} = \begin{bmatrix} \mathbf{x}_A^T \\ \mathbf{x}_\phi^T \end{bmatrix}, \quad (9)$$

where $\mathbf{x}_A = (r_q^2 + r_i^2)^{\frac{1}{2}}$ and $\mathbf{x}_\phi = \arctan(\frac{r_q}{r_i})$ denote the amplitude and phase vectors, respectively.

TABLE I
THE PROPOSED CNN LAYOUT FOR THE DATASET OF CASE1.

| Layer | Output Dimensions |
|----------------|----------------------------|
| Input | 8193×16 |
| Conv1 | $8193 \times 16 \times 64$ |
| Leaky ReLU1 | $8193 \times 16 \times 64$ |
| Max_Pool1 | $4097 \times 8 \times 64$ |
| Conv2 | $4097 \times 8 \times 128$ |
| Leaky ReLU2 | $4097 \times 8 \times 128$ |
| Max_Pool2 | $2049 \times 4 \times 128$ |
| Conv3 | $2049 \times 4 \times 64$ |
| Leaky ReLU3 | $2049 \times 4 \times 64$ |
| Max_Pool3 | $1025 \times 2 \times 64$ |
| Flatten | 131200 |
| Dense1 | 256 |
| Dense2 | 4 |
| Trainable Par. | 33, 736, 772 |

C. Fast Fourier Transform

The characteristics of signals in frequency domain can be employed as discriminating classification features. The FFT of the received signal is used to obtain a real-valued classification feature matrix \mathbf{X}_k^{FFT} as

$$\mathbf{f} = \mathcal{F}(r), \quad \mathbf{X}_k^{FFT} = \begin{bmatrix} \mathbf{f}_{re}^T \\ \mathbf{f}_{im}^T \end{bmatrix}, \quad (10)$$

where $\mathcal{F}(\cdot)$ stands for the FFT of the received signals; \mathbf{f}_{re} and \mathbf{f}_{im} are real and imaginary parts of \mathbf{f} , respectively.

D. Convolutional Neural Networks

CNN is a class of deep neural networks which is mainly employed in image classification and recognition. Still, it has been recently extended to several application areas. CNNs have two stages: feature extraction and classification. In feature extraction, a convolutional layer is followed by a pooling layer. In the convolution layer, the feature matrix is convolved with different filters to obtain convolved feature map as follows

$$h[i, j] = \sum_{p=1}^m \sum_{l=1}^n w_{p,l} \mathbf{X}_k[i+p-1, j+l-1], \quad (11)$$

where $w_{p,l}$ is the element at p -th row and l -th column of the $m \times n$ filter matrix, and $\mathbf{X}_k[\cdot, \cdot]$ denotes the elements of feature matrix convolved by $w_{p,l}$. The convolution layer is followed by the pooling layer to reduce computational complexity and training time, and control over-fitting due to the fact that pooling layer makes the activation less sensitive to feature locations [16]. The $u \times v$ maximum pooling operation is described as

$$g[i, j] = \max \{h[i+a-1, j+b-1]\}, \quad (12)$$

where $1 \leq a \leq u$ and $1 \leq b \leq v$. The output of the pooling layer is a 3-D tensor. This output is then reshaped into a 1-D vector. This vector is fed to the dense (fully-connected) layers for the final classification decision. The overall block diagram for the proposed CNN model is depicted in Fig. 5.

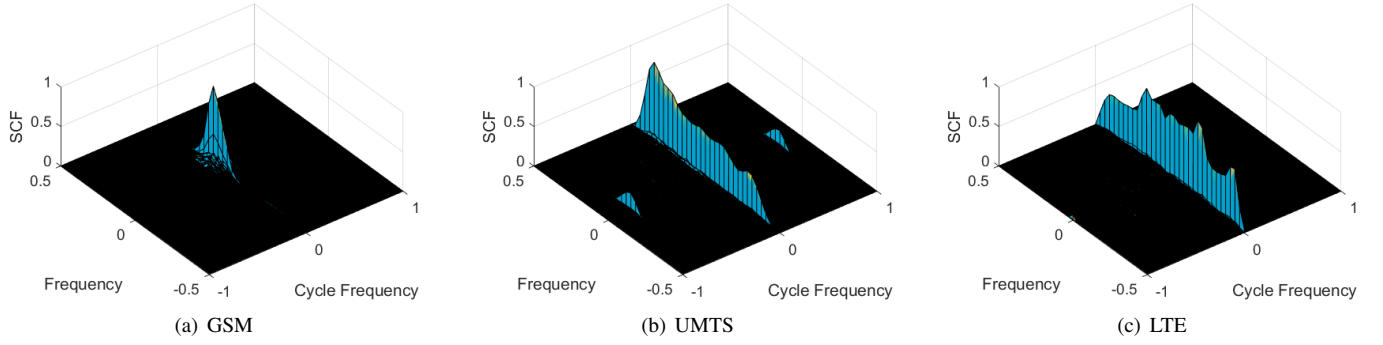


Fig. 2. SCFs in bi-frequency plane. They are estimated by FAM algorithm.

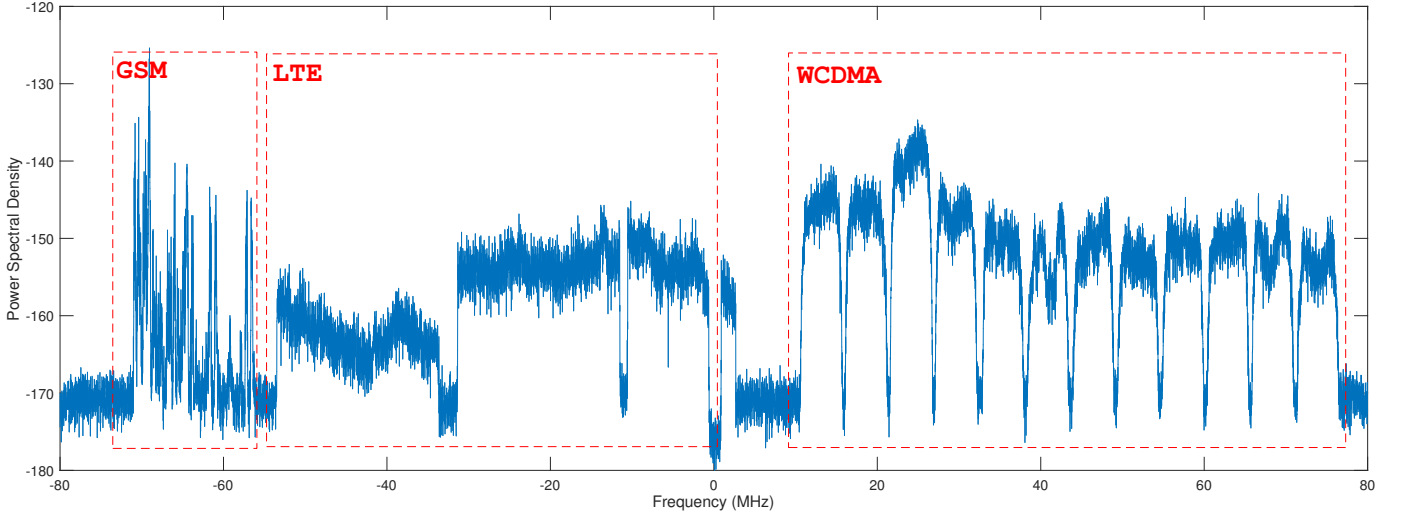


Fig. 3. The power spectrum of the signals in dataset. The spectrum is created by using different cellular communication bands.

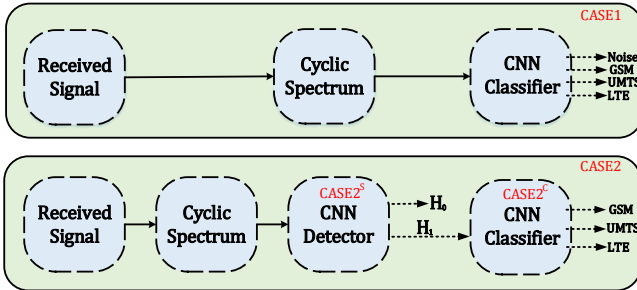


Fig. 4. Two different approaches for the sensing and classification of signals.

III. THE PROPOSED CNN MODEL

The construction of CNN for classification of wireless mobile communication signals is conducted via an open source machine learning library, Keras [17]. The designed CNN consists of three convolution and three pooling layers sequentially. The leaky rectified linear unit (ReLU) activation function with an alpha value 0.1 is used in each convolution layer to extract discriminating features. Leaky ReLU is selected instead of ReLU. Unlike ReLU, leaky ReLU maps larger negative values to smaller ones by a mapping line with a small slope. In each convolution layer, 3×3 filters are used. 2×2 max pooling

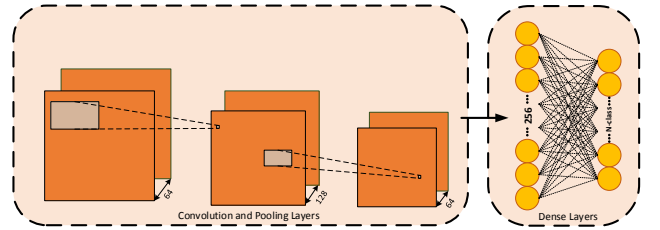


Fig. 5. The proposed CNN model consists of three convolutional layers and two dense layers with Adam optimizer with learning rate of 10^{-5} .

is used to reduce the dimension and training time. A fully connected layer is formed by 256 neurons and Leaky ReLU activation function. Following the fully connected layers, the probabilities for each class are computed by the softmax activation function. In addition, the adaptive moment estimation (ADAM) optimizer is utilized when determining the model parameters. In the training, early stopping is employed to avoid the model to overfit. All parameters are empirically tuned by considering the generalizability and performance of the proposed CNN model. The input matrices, \mathbf{X}_k^{AP} , \mathbf{X}_k^{FFT} , and \mathbf{X}_k^{SCF} are used at the beginning of the proposed model by convolving with filters.

It is customary to quantify the performance of a classifier model in terms of the precision (Π), recall (Ψ), and F_1 -score performance metrics. The precision metric quantifies how much positive results are actually positive, the recall provides information on how much true positives are identified correctly as positive, and F_1 -score gives an overall measure for the accuracy of a classifier model since it is the harmonic average of precision and recall. These metrics are given as

$$\Pi = \frac{\xi}{\xi + v}, \quad \Psi = \frac{\xi}{\xi + \mu}, \quad F_1\text{-score} = 2 \times \frac{\Pi \times \Psi}{\Pi + \Psi}, \quad (13)$$

where ξ , v , and μ denote the numbers of true positive, false positive, and false negative, respectively.

IV. PROBLEM STATEMENT

We consider two cases for the use of proposed CNN model:

CASE1: First, a CNN classifier based on the proposed model is trained with four different classes (*i.e.*, spectrum without any signal (AWGN), GSM, UMTS, and LTE). Then for a given frequency band as shown in Fig. 3, cyclic spectrum is constructed depending on the procedures described in Section II-A. The constructed cyclic spectrum is fed to the CNN classifier, which is already trained with four possible inputs. Finally, the classification is made.

CASE2: In this case a two-stage approach is adopted; at the first stage a CNN detector (the same CNN model defined in Section II-D is utilized for both detection and classification for the sake of simplicity) is utilized to decide whether a signal exists in the given band or not by training the CNN by two classed one comprised of GSM, UMTS, and LTE signals and the second AWGN. Thus in the first stage a decision is made about whether a signal exists in the spectrum or not as in the case of classical spectrum sensing. If the decision is made that there is an information bearing signal in the given band, second stage is activated utilizing a CNN classifier, which is trained with three classes (*i.e.*, GSM, UMTS, and LTE) and finally a decision is made for the class of the signal occupying the spectrum.

Please note that the classification refers to identification of the signals, and at the detection part of the approach H_1 and H_0 refers to the existence and non-existence of a signal over the spectrum based on binary hypothesis testing. Both CASE1 and CASE2 are illustrated in Fig. 4.

Firstly, we can define the accuracy for CASE1, P_{CASE1} as:

$$P_{\text{CASE1}} = P(\hat{\chi}_k = \chi_k), \quad k = 0, 1, 2, 3, \quad (14)$$

where χ_k denotes the label array of the transmitted signals and k represents the label of the classes AWGN, GSM, UMTS, and LTE, respectively. $\hat{\chi}_k$ is array for the predicted classes of the received signals. In a short, P_{CASE1} stands for the accuracy of four-classes classification problem. For CASE2, it is required to define two independent accuracy functions: the sensing accuracy, P_{CASE2}^S and the classification accuracy, P_{CASE2}^C , which are defined as

$$P_{\text{CASE2}}^S = P(\hat{\chi}_S = 1|H_1) + P(\hat{\chi}_S = 0|H_0), \quad (15)$$

$$P_{\text{CASE2}}^C = P(\hat{\chi}_k = \chi_k|H_1), \quad k = 1, 2, 3. \quad (16)$$

TABLE II
CLASSIFICATION PERFORMANCE METRICS FOR THE PROPOSED CNN MODEL WITH SCF, AP, AND FFT FEATURES FOR CASE2.

| SNR | Feature | Signal | Precision (Π) | Recall (Ψ) | F1-Score |
|------|---------|---------|---------------------|-------------------|----------|
| 1dB | AP | UMTS | 0.35 | 0.39 | 0.37 |
| | | LTE | 0.31 | 0.29 | 0.30 |
| | | GSM | 0.30 | 0.29 | 0.30 |
| | | Average | 0.32 | 0.32 | 0.32 |
| | FFT | UMTS | 0.00 | 0.00 | 0.00 |
| | | LTE | 0.21 | 0.50 | 0.30 |
| | | GSM | 0.00 | 0.00 | 0.00 |
| | | Average | 0.07 | 0.17 | 0.10 |
| | SCF | UMTS | 0.59 | 0.40 | 0.48 |
| | | LTE | 0.68 | 0.46 | 0.54 |
| | | GSM | 0.62 | 0.98 | 0.76 |
| | | Average | 0.63 | 0.61 | 0.59 |
| 5dB | AP | UMTS | 0.43 | 0.42 | 0.42 |
| | | LTE | 0.39 | 0.43 | 0.41 |
| | | GSM | 0.61 | 0.56 | 0.58 |
| | | Average | 0.47 | 0.47 | 0.47 |
| | FFT | UMTS | 0.53 | 0.49 | 0.51 |
| | | LTE | 0.25 | 0.51 | 0.34 |
| | | GSM | 0.00 | 0.00 | 0.00 |
| | | Average | 0.26 | 0.33 | 0.28 |
| | SCF | UMTS | 0.97 | 0.92 | 0.94 |
| | | LTE | 0.92 | 0.95 | 0.94 |
| | | GSM | 0.98 | 1.00 | 0.99 |
| | | Average | 0.96 | 0.96 | 0.96 |
| 10dB | AP | UMTS | 0.50 | 0.52 | 0.51 |
| | | LTE | 0.50 | 0.53 | 0.52 |
| | | GSM | 0.88 | 0.79 | 0.83 |
| | | Average | 0.63 | 0.61 | 0.62 |
| | FFT | UMTS | 0.49 | 0.37 | 0.42 |
| | | LTE | 0.27 | 0.62 | 0.38 |
| | | GSM | 0.00 | 0.00 | 0.00 |
| | | Average | 0.26 | 0.33 | 0.27 |
| | SCF | UMTS | 1.00 | 0.96 | 0.98 |
| | | LTE | 0.96 | 0.99 | 0.98 |
| | | GSM | 1.00 | 1.00 | 1.00 |
| | | Average | 0.99 | 0.98 | 0.98 |
| 15dB | AP | UMTS | 0.55 | 0.54 | 0.55 |
| | | LTE | 0.55 | 0.57 | 0.56 |
| | | GSM | 0.94 | 0.93 | 0.94 |
| | | Average | 0.68 | 0.68 | 0.68 |
| | FFT | UMTS | 0.73 | 0.49 | 0.58 |
| | | LTE | 0.35 | 0.82 | 0.49 |
| | | GSM | 0.00 | 0.00 | 0.00 |
| | | Average | 0.36 | 0.44 | 0.36 |
| | SCF | UMTS | 1.00 | 0.97 | 0.99 |
| | | LTE | 0.97 | 0.99 | 0.98 |
| | | GSM | 0.99 | 1.00 | 1.00 |
| | | Average | 0.99 | 0.99 | 0.99 |

$\hat{\chi}_S$ is the prediction regarding to presence of a signal in the spectrum. χ_k is the predictions for the classification part of CASE2. χ_S is defined for the transmitted signal as:

$$\chi_S = \begin{cases} 0, & k = 0, \\ 1, & k = 1, 2, 3. \end{cases} \quad (17)$$

The overall accuracy for CASE2 can be introduced in terms of P_{CASE2}^S and P_{CASE2}^C by

$$P_{\text{CASE2}} = P_{\text{CASE2}}^S P_{\text{CASE2}}^C. \quad (18)$$



Fig. 6. An overview of the measurement area. The transmitters are located in the urban area, but the receivers are in a sub-urban area.

V. DATASET GENERATION

The dataset has been created by preparing a measurement campaign. The measurements has been taken in different locations and bands. Fig. 6 denotes the locations of transmitters and receivers on the measurement area. The signals propagate through the urban area, and then reach the receivers in sub-urban area. The measurement focuses on 800, 900, 1800, and 2100 bands. These bands cover all cellular communication spectrum. In the receiver side, Rohde Schwarz FSW26 spectrum analyzer and Yagi-Uda antenna have been employed. For each signal, 16384 I/Q samples have been recorded. Totally, 60000 signals are included by the dataset. These signals have 15 different SNR levels. Each level consists of the same number of signals as 4000. The dataset is split into test and train data with the proportion of 0.4 and 0.6, respectively.

The wireless propagation channels are different as seen in Fig. 7. The received power and phase of the signals are affected by the shadowing, multipath fading and path loss. The figure denotes that the received signals have different power as well as different amplitude levels. Also, the distribution of the received power changes for each recorded signal since the measurements have been taken at different locations and time for various bands. Furthermore, Fig. 8 illustrates the phase distribution of the received signals. It is seen that the phase of received signals are distributed almost uniformly in between $-\pi$ and π radians. These samples give the impression of Rayleigh-like fading behavior due to amplitude and phase distributions of received signals. This result is expected when considering the measurement area and the locations of transmitters and receivers.

We want to emphasize that the dataset does not include bandwidth and carrier frequency of any signal as a feature. Thus, this dataset allows cognitive radios to perform opportunistically in any region of the spectrum.

The dataset is shared in [14] in the format of SCF, which is the main method used in this study. Since we used 16384 I/Q samples, the data dimension is 8193×16 for each signal.

VI. CLASSIFICATION PERFORMANCE ANALYSIS

We evaluate the performance of the proposed classification model as tested over a comprehensive dataset of wireless mobile communications signal. Our dataset is composed of

GSM, wideband code division multiple access (WCDMA) for UMTS and LTE signals which are recorded over-the-air at the different locations with unique conditions in terms of the number of channel taps, and fading, as noted in Section V. Sample power spectra of these signal types, obtained with the Welch's method, are shown in Fig. 3. Training and test sets contain 9000 and 6000 signals for each waveform. The I/Q signal length is 16384. CNN is trained and tested on a workstation computer with Intel Xeon(R) CPU E5 – 2630v3@2.40GHz \times 16 central processing unit (CPU), 64GB RAM and GeForce GTX 1070 graphics processing unit (GPU). The average training time per epoch is approximately 18s for SCF feature where both FFT and AP take 2.3s per epoch; however, both FFT and AP cannot show an acceptable classification performance, P_{CASE2}^C .

Firstly, we focus on the results for CASE1. As stated before, CASE1 refers to four-classes classification problem. As shown in Fig. 9, the test accuracy of the model exceeds 90% at 11dB SNR. It takes a maximum accuracy value of 92% at 15dB. The confusion matrices related to CASE1 are depicted in Fig. 10. At low SNR levels, the model mostly recognizes the signals such that there is no signal in the spectrum. This situation is viewed in Fig. 10(a). This phenomena calls an idea to divide the problem into two parts: firstly sense, then classify. In this case, we analyse both CNN detector and CNN classifier (see Fig. 4). For the sensing part of the architecture, noise signals are labeled as 0 and the rest of the set is labeled as 1. The detection results are plotted in Fig. 9. The detection accuracy follows 96% at almost all SNR values.

By assuming the signal is present in the spectrum, it is investigated how the CNN classifier performs in the classification part of CASE2. At this stage, it is observed that the classification accuracy exceeds 90% at 3dB SNR. It gives the best performance, 98.5%, at 9dB and it is remained up to 15dB. It is seen in Fig. 11(a) that even at low SNR regime, the classifier can identify GSM signals with high accuracy; however, the precision is low. Unlike GSM signals, the classifier has difficulty in recognition of UMTS and LTE signals. It is clearly observed in Fig. 11(b) and Fig. 11(c) that both the accuracy and precision of the classifier enhance as the SNR value increases.

As seen in Fig. 9, the CNN-based classifier shows a superior performance compared to SVM-based classifier, which has been proposed in our previous work [13], under the conditions of the classification part of CASE2. The CNN-based classifier both employs less costly feature due to omitting bi-frequency mapping and performs with higher accuracy than SVM classifier.

The results for CASE2 were given up to this point in parts. Now, we can examine the overall performance of CASE2. Obviously, there is a loss of performance due to some misdetection in the sensing phase. Both the detection rate in the sensing stage and the accuracy in the classification stage are high at 3dB and thereafter, so overall performance does not suffer a significant loss. As shown in Fig. 9, the overall performance of CASE2 is far superior to that of CASE1. Especially at low SNR levels, the signals remaining after first detecting and separating noise from the signal set by the CNN

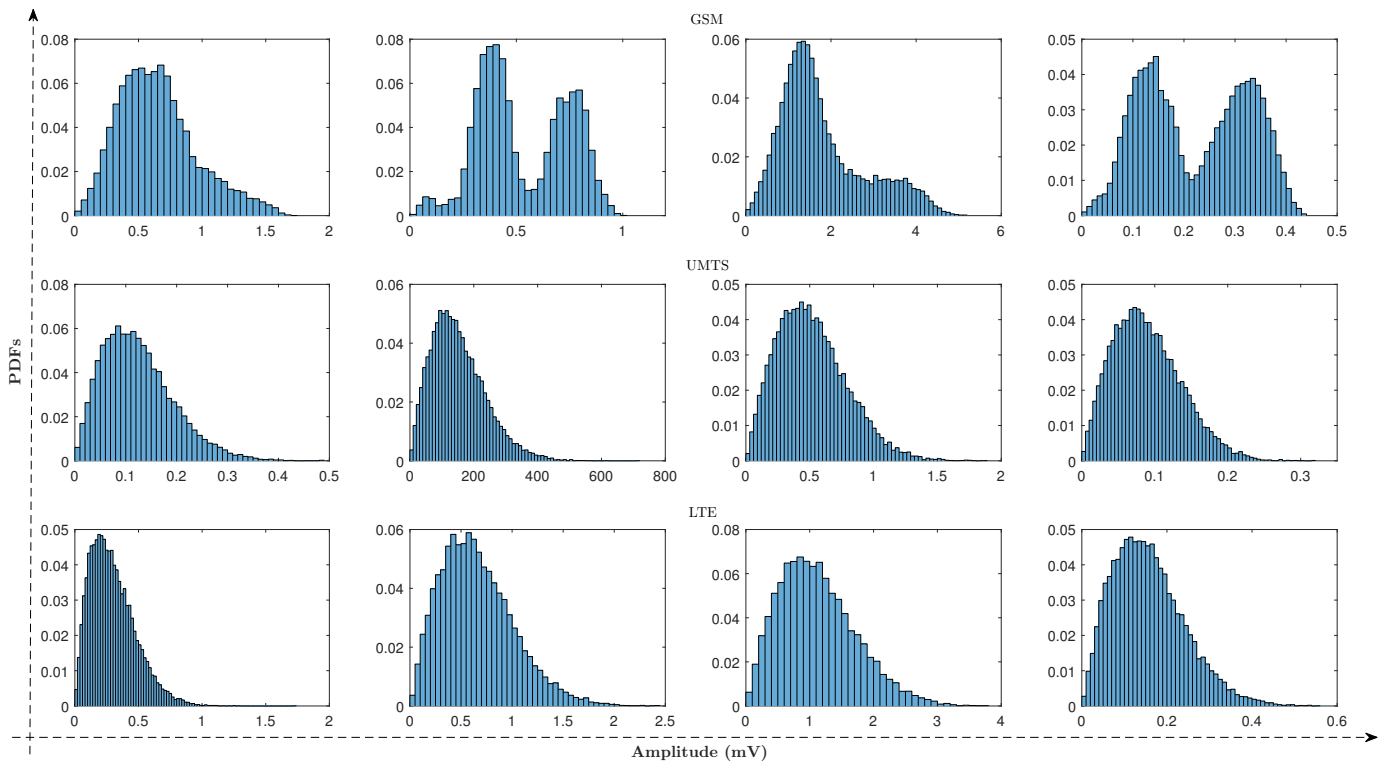


Fig. 7. Sample PDFs of the amplitude of received signals in the dataset. The example PDFs show the difference channel and received power characteristics.

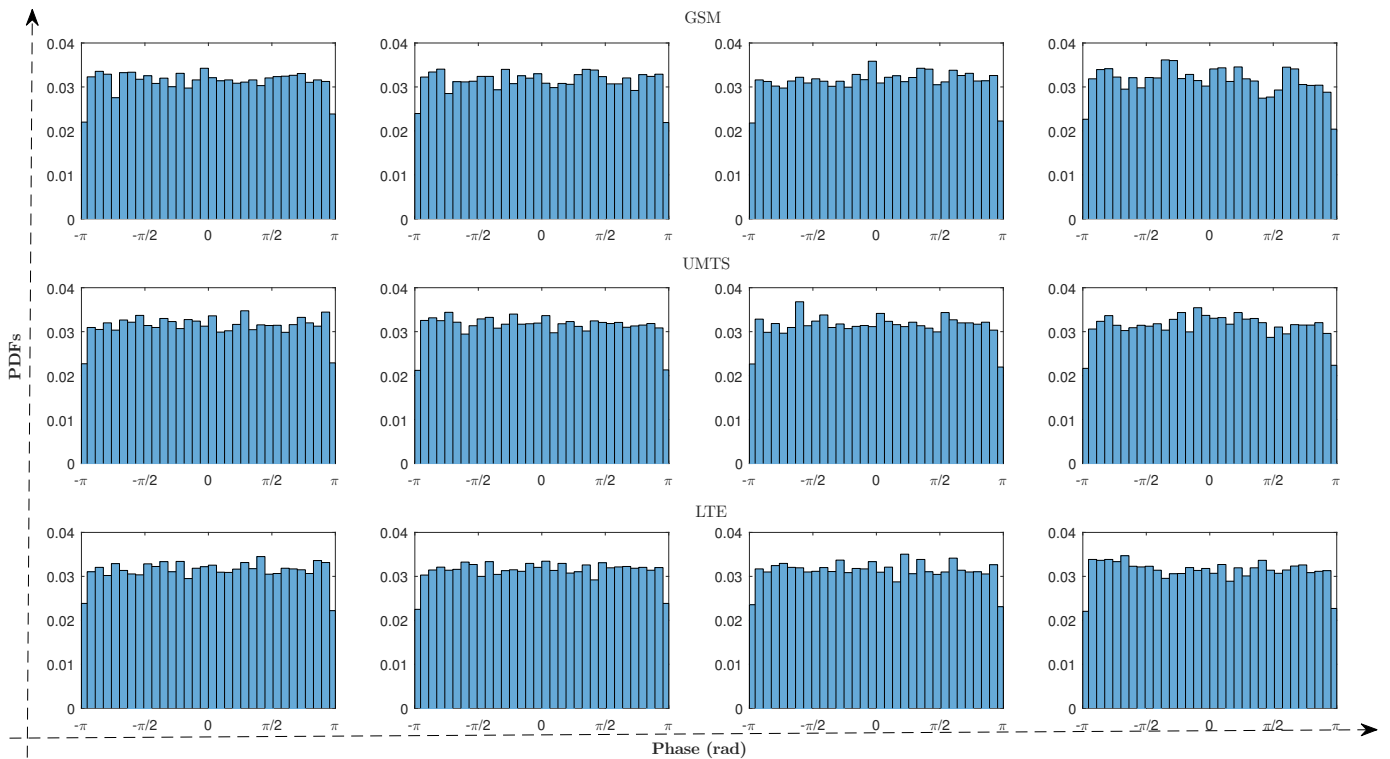


Fig. 8. Sample PDFs of the phase of received signals in the dataset. The example PDFs show uniform distribution characteristics.

detector can be classified with much better performance. In this way, the performance is higher in CASE2. However, it should be noted that CASE2 is more costly than CASE1 in terms of training time and the number of models. Obviously,

CASE2 can be predicted to perform much better than CASE1 in the presence of a jammer or interference signal which they show Gaussian characteristics.

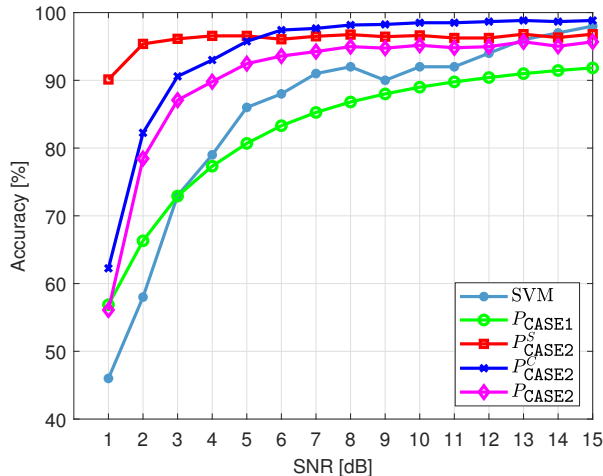


Fig. 9. Accuracy values with respect to SNR level of the received signals for both cases.

A. Investigation of the Impact of Different Features

Furthermore, we compare the performance of features AP and FFT with SCF. The features are used as detailed in Section II. The results of this test are presented in Table II. The average performances also indicate that SCF outperforms FFT and AP for all SNR levels. Assuming that these two are used along with I/Q as the main features for training, these results show significant gains for real-world signals especially above 5dB SNR level. It is observed that AP performs better than FFT. Although the cost of computing both features is far behind the SCF, they are far from delivering the desired performance. In our previous study [13], the analysis based on t-distributed stochastic neighbor embedding (t-SNE) results showed that SCF better separates signal vectors in space. The results of this study are in line with the previous analysis.

B. Comparison with A Classical Method

Besides signal classification, the proposed CNN model can be used for spectrum sensing. We investigated the sensing performance of the model by training a CNN-based spectrum occupancy detector trained over 600 pure noise signals and 600 noisy WCDMA signals for each SNR value. Then, the model is tested with 400 pure noise signals and 400 noisy WCDMA signals for each SNR level and sensing results are acquired. Furthermore, for comparison purposes, we implement a CFAR detector utilizing classical CFD [18] to identify WCDMA signals and the same dataset is also used for CFAR detector. Please note that UMTS signals are deliberately selected due to their known dominant SCF characteristics stemming from cyclic spreading codes. The results of this test are given in Fig. 12. In view of these results, it is clearly seen that the CNN-based detector outperforms the CFAR detector at all SNR regimes. For example, the sensing performance of the CNN-based detector is 91.75% at 3dB while the probability of detection for the CFAR detector are 45.6% and 59.4% for the selected false alarm rates as 0.05 and 0.1, respectively.

TABLE III
PERFORMANCE COMPARISON BETWEEN THE EXISTING DL NETWORKS AND THE PROPOSED SYSTEM FOR THE CLASSIFICATION STAGE OF CASE2 AT SNR VALUE OF 15DB.

| Network | Signal | Precision | Recall | F_1 -score |
|--------------|---------|-----------|--------|--------------|
| CLDNN [19] | UMTS | 0.33 | 1.00 | 0.50 |
| | LTE | 0.00 | 0.00 | 0.00 |
| | GSM | 0.00 | 0.00 | 0.00 |
| | Average | 0.11 | 0.33 | 0.17 |
| LSTM [20] | UMTS | 0.33 | 1.00 | 0.50 |
| | LTE | 0.00 | 0.00 | 0.00 |
| | GSM | 0.00 | 0.00 | 0.00 |
| | Average | 0.11 | 0.33 | 0.17 |
| CNN with SCF | UMTS | 0.79 | 1.00 | 0.88 |
| | LTE | 1.00 | 0.72 | 0.84 |
| | GSM | 0.99 | 1.00 | 0.99 |
| | Average | 0.93 | 0.91 | 0.91 |

C. Comparison with Existing Deep Learning Networks

The existing DL networks are employed to classify the cellular communication signals. We employed convolutional long short term memory fully connected deep neural network (CLDNN) [19] and LSTM [20] models. These models are originally used in modulation classification. Without any change in the models, input matrix, and input vector as proposed in the papers are employed in the study. CLDNN takes a 2×128 matrix which composes of amplitude and phase values for each I/Q sample. On the other hand, LSTM model utilizes a vector reshaped version of the matrix used in CLDNN. Therefore, the length of the vector is 256. Its first half includes in-phase components while the rest of the vector is quadrature components. Other details are found in [19, 20]. The precision, recall, and F_1 -score are given in Table III. It shows that CLDNN and LSTM decide that the received signal is UMTS whatever it actually is. Even though LSTM and CLDNN can be trained in a short time by using I/Q vector and matrix, using I/Q vector and matrix give poor classification performance.

VII. CONCLUSION

In this study, two approaches are introduced to sense and identify cellular communication signals. Firstly, an approach investigated for joint sensing and classification. The test results exhibit that two steps approach performs better than the joint approach. Furthermore, test results that are based on real-world measurements indicate SCF as a superior feature for the identification of wireless mobile communications signals for DL models. Moreover, under the stringent channel condition, CNN provides better spectrum sensing performance than classical CFD without using any a priori information. These results imply that the utilization of DL networks in cognitive radio technology allows a more robust system design. In subsequent studies, the performance of the model proposed in this study can be examined against adversarial attacks and efforts can be made to develop various methods to strengthen its resistance to this type of attack.

REFERENCES

- [1] W. A. Gardner, "Exploitation of spectral redundancy in cyclostationary signals," *IEEE Signal Process. Mag.*, vol. 8, no. 2, pp. 14–36, Apr. 1991.

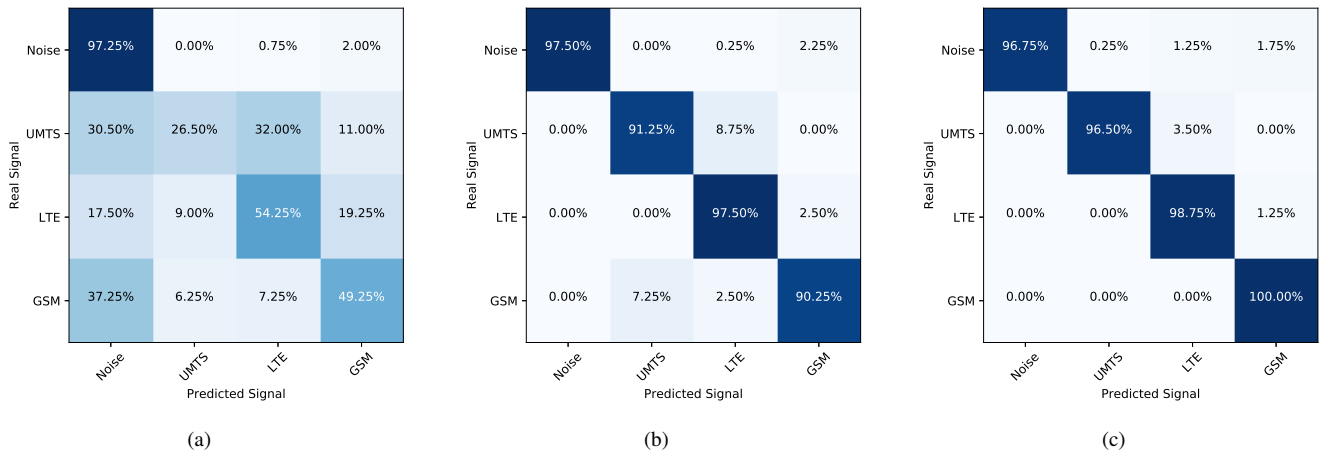


Fig. 10. Confusion matrices for CASE1 at SNR levels of (a) 1dB, (b) 5dB, and (c) 10dB.

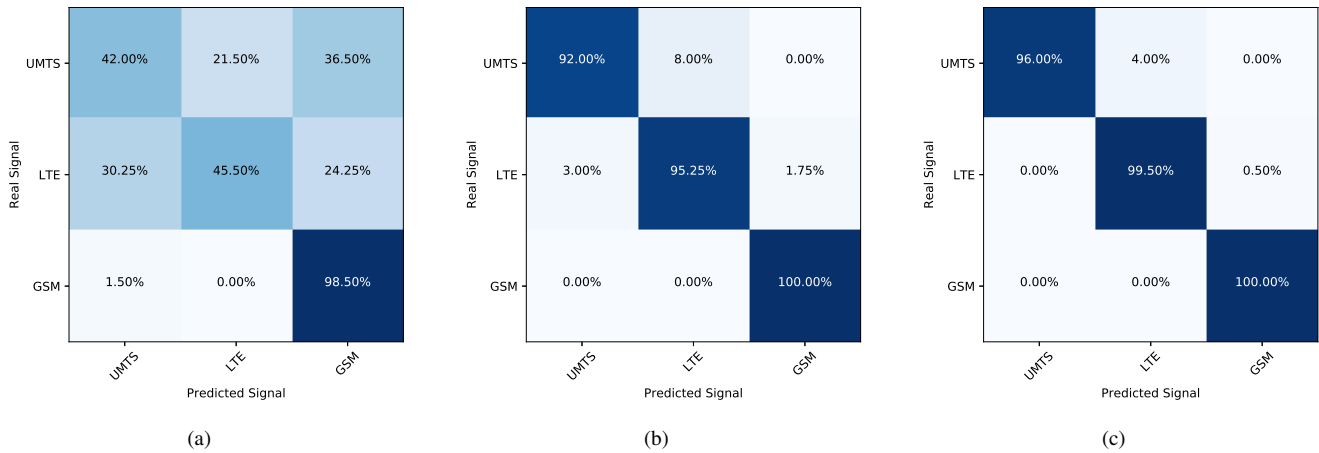


Fig. 11. Confusion matrices for the classification part of CASE2 at SNR levels of (a) 1dB, (b) 5dB, and (c) 10dB.

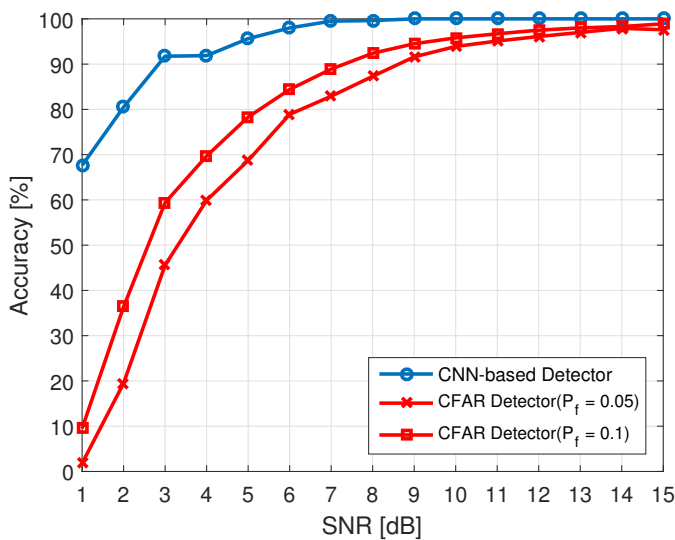


Fig. 12. Spectrum sensing performances of CFAR detectors and CNN-based detector with respect to SNR.

[2] M. Oner and F. Jondral, "Air interface identification for software radio

systems," *AEU - Intl. J. Electron. Commun.*, vol. 61, no. 2, pp. 104–117, 2007.

[3] E. Karami, O. A. Dobre, and N. Adnani, "Identification of GSM and LTE signals using their second-order cyclostationarity," in *Proc. IEEE Int. Instrum. Meas. Tech. Conf.*, Pisa, Italy, May. 2015, pp. 1108–1112.

[4] Y. A. Eldemerdash, O. A. Dobre, O. Ureten, and T. Yensen, "Identification of cellular networks for intelligent radio measurements," *IEEE Trans. Instrum. Meas.*, vol. 66, no. 8, pp. 2204–2211, Apr. 2017.

[5] A. Hazza, M. Shoaib, S. A. Alshebeili, and A. Fahad, "An overview of feature-based methods for digital modulation classification," in *Proc. Intl. Commun. Signal Process., and Their Applications*, Mar. 2013.

[6] W. M. Lees, A. Wunderlich, P. Jeavons, P. D. Hale, and M. R. Souryal, "Deep learning classification of 3.5 GHz band spectrograms with applications to spectrum sensing," *IEEE Trans. Cogn. Commun. Netw.*, 2019.

[7] T. J. O'Shea, T. Roy, and T. C. Clancy, "Over-the-air deep learning based radio signal classification," *IEEE J. Sel. Signal Process.*, vol. 12, no. 1, pp. 168–179, Jan. 2018.

[8] M. Kulin, T. Kazaz, I. Moerman, and E. D. Poorter, "End-to-end learning from spectrum data: A deep learning approach for wireless signal identification in spectrum monitoring applications," *IEEE Access*, vol. 6, pp. 18 484–18 501, Mar. 2018.

[9] S. Kokalj-Filipovic, R. Miller, and J. Morman, "AutoEncoders for training compact deep learning RF classifiers for wireless protocols," *arXiv preprint arXiv:1904.11874*, 2019.

[10] S. Rajendran, W. Meert, D. Giustiniano, V. Lenders, and S. Pollin, "Deep learning models for wireless signal classification with distributed low-cost spectrum sensors," *IEEE Trans. Cogn. Commun. Netw.*, vol. 4, no. 3, pp. 433–445, May. 2018.

- [11] H. Xia, K. Alshathri, V. B. Lawrence, Y.-D. Yao, A. Montalvo, M. Rauchwerk, and R. Cupo, "Cellular signal identification using convolutional neural networks: Awgn and rayleigh fading channels," in *IEEE International Symposium on Dynamic Spectrum Access Networks*, 2019, pp. 1–5.
- [12] S. Kokalj-Filipovic, R. Miller, and J. Morman, "Targeted adversarial examples against RF deep classifiers," in *Proceedings of the ACM Workshop on Wireless Security and Machine Learning*, 2019, pp. 6–11.
- [13] K. Tekbıyık, Ö. Akbunar, A. R. Ekti, A. Görçin, and G. K. Kurt, "Multi-dimensional wireless signal identification based on support vector machines," *IEEE Access*, vol. 7, pp. 138 890–138 903, 2019.
- [14] —, "COSINE: Cellular cOmmunication SIgNal dataseT," 2020. [Online]. Available: <http://dx.doi.org/10.21227/safr-gh59>
- [15] R. Roberts, W. Brown, and H. Loomis, "Computationally efficient algorithms for cyclic spectral analysis," *IEEE Signal Process. Mag.*, vol. 8, no. 2, pp. 38–49, Apr. 1991.
- [16] M. D. Zeiler and R. Fergus, "Stochastic pooling for regularization of deep convolutional neural networks," *arXiv preprint arXiv:1301.3557*, 2013.
- [17] F. Chollet *et al.*, "Keras," <https://keras.io>, 2015.
- [18] C. M. Spooner and A. N. Mody, "Wideband cyclostationary signal processing using sparse subsets of narrowband subchannels," *IEEE Trans. on Cogn. Commun. Netw.*, vol. 4, no. 2, pp. 162–176, 2018.
- [19] Ramjee, Sharan and Ju, Shengtai and Yang, Diyu and Liu, Xiaoyu and Gamal, Aly El and Eldar, Yonina C, "Fast deep learning for automatic modulation classification," *arXiv preprint arXiv:1901.05850*, 2019.
- [20] Hu, Shisheng and Pei, Yiyang and Lianul Pu and Liang, Ying-Chang, "Robust modulation classification under uncertain noise condition using recurrent neural network," in *IEEE Glob. Commun. Conf.*, 2018, pp. 1–7.

Kürşat Tekbıyık (S'19) received his B.Sc. degree (with high honors) in electronics and communication engineering from Istanbul Technical University, Istanbul, Turkey, in 2017. He also received M.Sc. degree in telecommunication engineering from Institute of Science at Istanbul Technical University in 2019. He is currently pursuing his Ph.D. degree in the same programme. He is employed by The Scientific and Technological Research Council of Turkey at Informatics and Information Security Research Center. He is the author of several publications



and he worked in projects aiming secure communication. He was with Aselsan Inc., where he worked on system design of ground terminals for satellite communication. His research interests include algorithm design for signal intelligence, next-generation wireless communication systems, terahertz wireless communications, and machine learning.

Özkan Akbunar received B.Sc. degree from Electrical and Electronics Engineering department in Anadolu University, Eskişehir, TURKEY. He is proceeding his M.Sc education in Telecommunication Engineering department in Istanbul Technical University, Istanbul, Turkey. He is working in The Scientific and Technological Research Council of Turkey at Informatics and Information Security Research Center as R&D engineer since December 2017. His main research areas are wireless communication systems, digital signal processing, machine



learning and radar.



Ali Rıza Ekti is from Tarsus, Turkey. He received B.Sc. degree in Electrical and Electronics Engineering from Mersin University, Mersin, Turkey, (September 2002-June 2006), also studied at Universidad Politecnica de Valencia, Valencia, Spain in 2004-2005, received M.Sc. degree in Electrical Engineering from the University of South Florida, Tampa, Florida (August 2008-December 2009) and received Ph.D. degree in Electrical Engineering from Department of Electrical Engineering and Computer Science at Texas A&M University (August 2010-August 2015). He is currently an assistant professor at Balıkesir University Electrical and Electronics Engineering Department and also senior researcher at TUBITAK BILGEM. His current research interests include statistical signal processing, convex optimization, machine learning, resource allocation and traffic offloading in wireless communications in 4G and 5G systems and smart grid design and optimization.

PLACE
PHOTO
HERE

Ali Görçin graduated from Istanbul Technical University with B.Sc. in Electronics and Telecommunications Engineering and completed his master's degree on defense technologies at the same university. After working at Turkish Science Foundation (TUBITAK) on avionics projects for more than six years, he moved to the U.S. to pursue PhD degree in University of South Florida (USF) on wireless communications. He worked for Anritsu Company during his tenure in USF and worked for Reverb Networks and Viavi Solutions after his graduation.

He is currently holding an assistant professorship position at Yıldız Technical University in Istanbul and also serving as the vice president of Informatics and Information Security Research Center of TUBITAK, responsible from testing and evaluation along with research and development activities on wireless communications technologies.

Güneş Karabulut Kurt received the B.S. degree (with honors) in electronics and electrical engineering from Bogazici University, Istanbul, Turkey, in 2000 and the M.A.Sc. and Ph.D. degrees in electrical engineering from the University of Ottawa, Ottawa, ON, Canada, in 2002 and 2006, respectively. From 2000 to 2005, she was a Research Assistant with the CASP Group, University of Ottawa. Between 2005 and 2006, she was with TenXc Wireless, where she worked on location estimation and radio frequency identification systems. From 2006 to 2008, she was



with Edgewater Computer Systems Inc., where she worked on high-bandwidth networking in aircraft and priority-based signaling methodologies. From 2008 to 2010, she was with Turkcell R&D Applied Research and Technology, Istanbul. Since 2010, she has been with Istanbul Technical University, where she is currently a full Professor. Dr. Karabulut Kurt is a Marie Curie Fellow and her project REALMARS is selected to be a success story by European Commission Research Executive Agency. She is the author of numerous publications and international patents. Dr. Karabulut was involved in various research projects including STREP, EUREKA and ITEA-2 projects on wireless networks. She served a management committee member of the COST Action 1104.